FINITE ELEMENT ANALYSIS TO QUANTIFY THE EFFECT OF SURGERY IN PROXIMAL FEMUR

Basil Mathai

FINITE ELEMENT ANALYSIS TO QUANTIFY THE EFFECT OF SURGERY IN PROXIMAL FEMUR

Thesis submitted in partial fulfillment
of the requirement for the degree

of

Master in Technology

in
Biomedical Engineering

by

Basil Mathai

213BM1010

Under the supervision of

Dr. A Thirugnanam

DEPARTMENT OF BIOTECHNOLOGY AND MEDICAL ENGINEERING

NATIONAL INSTITUTE OF TECHNOLOGY, ROURKELA

MAY 2015

DEPARTMENT OF BIOTECHNOLOGY AND MEDICAL ENGINEERING

NATIONAL INSTITUTE OF TECHNOLOGY, ROURKELA

CERTIFICATE

This is to certify that the thesis entitled **"Finite element analysis to quantify the effect of surgery in proximal femur",** submitted by **Basil Mathai (Roll no. 213bm1010)** to National Institute of Technology, Rourkela, is a record of bonafide research work under my supervision and I consider it worthy of consideration for the award of the degree of Master of Technology of the Institute.

Place : NIT Rourkela
Date : 30 May 2015

Dr. A Thirugnanam
Assistant Professor
Department of Biotechnology & Medical Engineering
National Institute of Technology
Rourkela, 769008

DECLARATION

I certify that

1. The work contained in the thesis is original and has been done by myself under the general supervision of my supervisor.
2. The work has not been submitted to any other Institute for any degree or diploma.
3. I have followed the guidelines provided by the Institute in writing the thesis.
4. Whenever I have used materials (data, theoretical analysis, and text) from other sources, I have given due credit to them by citing them in the text of the thesis and giving their details in the references.

Basil Mathai

ACKNOWLEDGMENTS

The work that follows is by far the most memorable and notable in my life and no amount of thanks could be delivered to the people who have helped me create and document it. Still, I would take this opportunity to show my sincere gratitude towards my supervisor, Dr. A Thirugnanam. Without him this work would not have been what it is now. The long discussions and longer debates with him has not only helped me make this work noteworthy but also help me understand various aspects of life. I am also indebted to my father, Mathai who inspired me to take a new challenge in life which I thoroughly enjoyed and will always cherish. I would also like to thank all my lab-mates and my friends.

Date : 30 May 2015
Place : NIT Rourkela

Basil Mathai

Contents

List of Figures

List of Tables

List of Symbols and Abbreviations

$3GCF$	Third generation composite femur
BEL	Biomechnics European Laboratory
BMD	Bone Mineral Density
BW	Body Weight
CAD	Computer-aided Design
F_i	Force along direction i (N)
FEA	Finite Element Analysis
FEM	Finite Element Method
$HCFs$	Hip Contact Forces
HRA	Hip Resurfacing Arthroplasty
PDE	Partial Differential Equation
$PMMA$	Poly(methyl methacrylate)
THA	Total Hip Arthroplasty

Subscript

x	direction along x-axis
y	direction along y-axis
z	direction along z-axis

Abstract

Stress shielding and subsequent implant loosening is a very common challenge in a total hip arthroplasty (THA) and hip resurfacing surgeries. Load path in the bone altered by implant need to be studied carefully to develop implants having long term success. Stress distribution in the proximal femur is found to produce mechanical stimuli which activate the mechanotransduction pathways to induce bone remodeling in surrounding region.

In current study, Computer aided (CAD) model of intact femur, implanted femur and femur bone with resurfacing cup were modeled to represent pre and post operating geometry. Finite element analysis was performed by imposing $3D$ muscle forces and hip contact force during normal activity. The von mises stress distribution in the geometries was calculated. Study reveals that the stress distribution in the proximal femur is strongly affected by the patient activity and surgical procedure. Predominant stress shielding was observed in implanted femur, especially in lateral region of trochanters. Resurfaced cup model found to retain the physiological load transfer across the femur.

Keywords: Finite element analysis, Computed aided design, stress shielding, proximal femur,total hip arthroplasty

CHAPTER 1

Introduction

1.1 Overview

The current study focuses on stress distribution of bone around the implant through computer simulations. Load path in the bone is altered by implants because of its design, material property and surgical procedure. Stress changes in the surrounding bone produced by surgeries found to be crucial. These mechanical stimuli activate the mechanotransduction pathways to induce bone remodeling in surrounding region.

Finite element analysis of the intact and implanted models of the femur help to understand the load transfer in the proximal femur. The left femur bone geometry is retrieved from BEL repository. The implant geometries of prosthesis and resurfacing cup is modeled in CAD software and virtually implanted in bone geometry. Finite element model for computer analysis is made by assigning mechanical properties of bone, biomaterial into elements. Imposing physiological loading condition from routine activities among THA patient is important to understand the long term success. The hip contact force and associated muscle force from daily activities among THA patients is used for analysis of the computer models. The results are fetched in chapter 4 and conclusions are drawn.

This chapter consists of overview and general information to navigate through thesis.

1.2 Background

1.2.1 Femur bone

The femur extending from the hip to the knee is the strongest and the longest bone in the human body. The long, vertical part of the femur is called the femoral shaft. Another important features of this bone includes the head, medial condyles, lateral condyles, patellar surface, medial and lateral epicondyles, greater trochanters and lesser trochanters (Figure 1.1). The head is where the bone forms the hip joint with the innominate bone. The condyles are the points of articulation with the lower leg bone, tibia. The patellar surface has a groove shape where the femur articulate with the patella, or knee cap. The epicondyles and trochanters are all important attachment sites for various muscles. The human femur difficult fractured that it can able to endure forces up to 11,000 Newton. A fracture in this bone can only result from a large amount of force arise from impact loading, such as during a car accident or a fall from an high altitudes. Such an injury can take few months to heal.

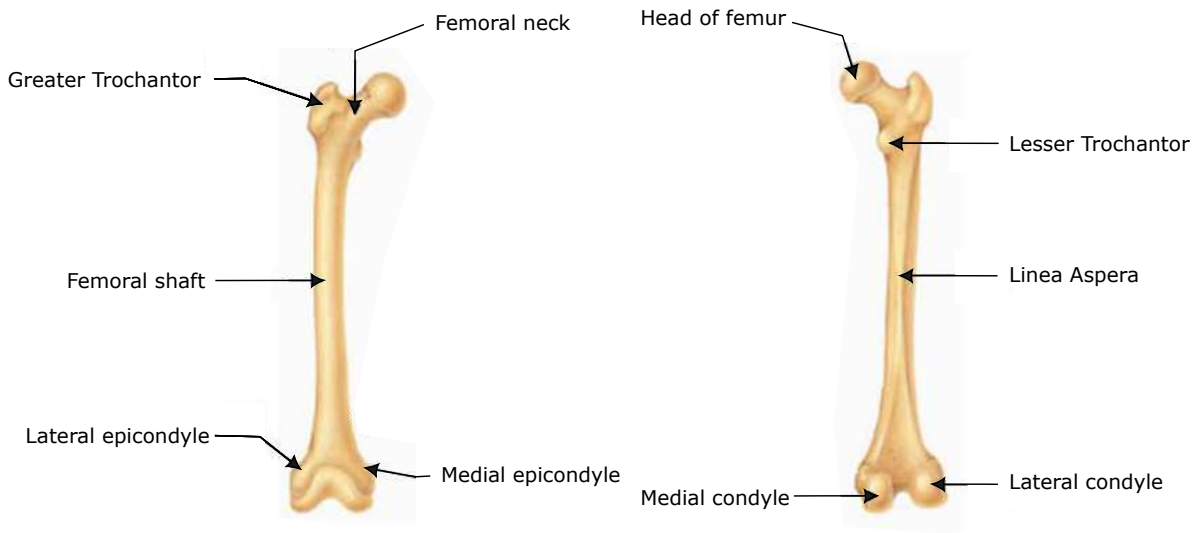

Figure 1.1: Anatomy of a human femur bone (thighbone).

Bone composed of two kinds of tissue; the outer part which is a dense compact tissue called cortex. The inner part cancellous tissue consists of lamellæ, which join to form a reticular structure. The compact tissue is found on the exterior of the bone, the cancellous in the interior [1]. Depending on different type of bones the relative quantity of these two kinds of tissue varies, from parts to parts. The formation of these tissue found to be governed by strength or lightness requisite [2]. Cortical bone (compact bone) facilitates main functions of bone: to support the whole body, protect organs, act as mechanical levers for movement, and store and release chemical elements, mainly

calcium. Compact bone is much denser than cancellous bone that it contributes about 80% of the weight of a human skeleton. Furthermore, it is harder, stronger and stiffer than cancellous bone. Osteon is the primary anatomical and functional unit of cortical bone were as trabecula is of cancellous bone.

Compared to compact bone, density of cancellous bone is lesser, and it posses a higher surface area to mass ratio. This gives raise to softer, weaker, and more flexible characteristics to cancellous bone. The large surface area in cancellous bone with cortical bone makes calcium ions exchange more efficient to support metabolic activity. Cancellous bone is normaly found at the proximal to joints within the interior of bone. Highly vascular cancellous bone contains red bone marrow where the blood cells haematopoiesis is produced [3]. It is scientifically proven that the trabecula within the cancellous bone is aligned in order to support the mechanical load that a bone experiences [4].

Proximal Extremity of the Femur

The portion of femur close to torso (proximal extremity) contains the head, neck, the two trochanters and adjacent structures [5].

The femur head is of spherical in shape articulates with the acetabulum of the pelvic bone. However it contains a small depression; fovea, connected through the round ligament to the sides of the acetabular notch. The head of the femur is linked to the shaft through the neck (collum). The neck is 3–5 cm long and approximately cylindrical in shape having smallest diameter from front to back and compressed in middle. The column forms an angle with the shaft at 130 degrees. This angle varies remarkably from population to population. It is also found that the average angle reduce from about 150 degrees in the infant to 120 degrees in old age. An abnormality related to increasing in the angle is known as coxa value and an exceptional decrease in angle is called coxa vara. Both the head and neck of the femur is vastly embedded in the hip musculature and can not be directly palpated. In lean people with thigh laterally rotated, the head of the femur can be felt deep as a resistance profound (deep) for the femoral artery [5].

The quadrate tubercle located on the intertrochanteric crest junction. The size of the tubercle varies and it is not always located on the intertrochanteric crest. The adjacent areas of the tubercle can be part of the quadrate tubercel, like the posterior surface of the greater trochanter or the neck of the femur. Anatomical study shows that the epiphysial line passes directly through the quadrate tubercle.

1.2.2 Forces acting on the hip joint

The hip joint is surrounded by large number of soft tissues including muscles and ligaments, which affect the forces acting on the femur head. Lack of knowledge about the

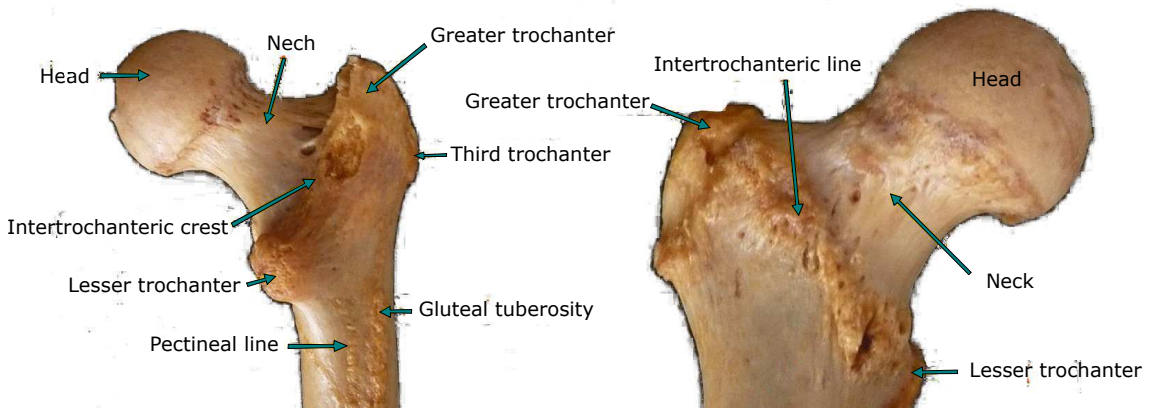

Figure 1.2: Upper extremity of left femur (a) Superior epiphysis - posterior view showing head, neck, greater trochanter, lesser trochanter and intertrochanteric line (b) Superior epiphysis - anterior view showing head, neck, greater trochanter, lesser trochanter, intertrochanteric crest and trochanteric fossa [5].

magnitude and direction of these forces in various activities makes the bio-mechanical analysis of hip joint difficult.

The force acting on the head of the femur will be about three times the total body weight. During the stance-phase, the hip contact force can reach upto 4.5 times the body weight considering the dynamic force. Along with hip contact force the muscle forces around the joint play important role in physiological loading. Determination of forces acting on the femoral head during walking is often combined with the gait analysis. It is often good practice to correlate the forces with the phases of gait. Besides from the static load, the dynamic forces are also involved in gait analysis. Therefore, gait may cause a load on the hip-joint will be considerably higher than the body weight. Hip loading can also be measured in vivo using instrumented prostheses [7, 8]. Musculoskeletal models can be employed to predict muscular forces and joint loading in a noninvasive way using inverse dynamic analysis [9, 10]. The Figure 1.3 model consists of 6 segments (pelvis, femur, patella, tibia, hindfoot and midfoot plus phalanxes) considered as rigid bodies onto which the muscles are attached. Lower limb musculoskeletal models usually validated against in vivo measured hip contact forces ($HCFs$) usually exhibit a tendency to overestimate the magnitude [11]. Its also found that the changes in joint geometry may results in the magnitude and orientation of the hip contact force vector during a gait cycle[6].

1.2.3 Hip surgery and implants

Prosthetic devices are being surgically implanted in the human body to replace the affected joint in order to restore its normal function. Total hip replacements were designed and used in patients in the first half of the 20th century onwards however, the initial results were not satisfactory. The main concerns includes, the implant design,the surface

Figure 1.3: A lower limb musculoskeletal model used for lower extremity study [6].

bearing materials of the metal-on-metal and the metal-on-polymer femoral-acetabular component types. The Swedish Total Hip Replacement Register is an excellent publication which incorporates very important clinical results of implant survival. It considers cemented, cementless, and hybrid implants with different designs in patients due to aseptic loosening [12].

Total total hip arthroplasty (THA)

Hip replacement surgery can be either performed as a total replacement or a hemi replacement. A total total hip arthroplasty (THA) comprise of replacing both the acetabulum and the femoral head while hemi arthroplasty generally replaces only the femoral head. The femoral head is removed and replaced with a prosthetic ball made of metal or ceramic and the socket (acetabulum) is replaced with a prosthetic cup. The cup generally consists of one or two components made of metal, ceramic or plastic.

Implant designs in early days had the potential to loosen from their attachment to the bones, typically becoming painful ten to twelve years after placement. Erosion and density degradation of the bone around the implant was observed on x-rays. Some device provided with a small holes in the stem into which bone graft was placed before

implanting the stem. This practice anticipated the bone in growth through the window over time and hold the implant in position.

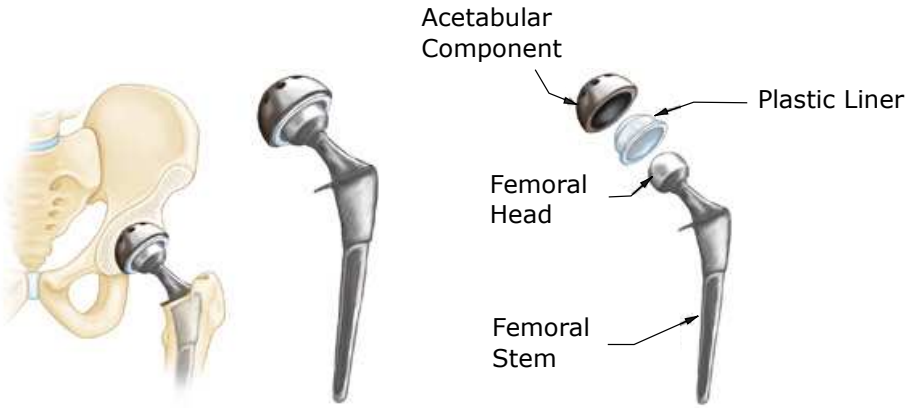

Figure 1.4: A schematic representing a left hip has been replaced, with the ball of this ball-and-socket joint replaced by a metal head that is set in the femur and the socket replaced by a metallic cup .

Arthritis is one of the situations where joint replacements are often required. Arthritis is a condition usually associated with old age in which the cartilage at joints wears away, results in the bones at joints rub against each other, causing pain and minimized mobility. Additionally, as people get older, their bones become more brittle. Increased bone loss (osteoporosis) also leaves them with an increased risk of a hip fracture.

Currently cemented stems tend to have a better length of service than uncemented stems. Uncemented stems are selected for patients with good bone health that can resist the forces and torque imposed on it. Cemented devices are typically selected for patients with poor bone quality who are at risk of fracture during stem insertion. Manufacturing cost of cemented stems are less, but good surgical practice is needed to fix them. One in every five patients have reported pain with activity during the first year after placement in case of uncemented stems. This must be due to the bone adaptation to the device. However fixation by the ingrowth of bone gave better clinical results [13].

Hip resurfacing arthroplasty (HRA)

Hip resurfacing has been developed as a surgical alternative to total hip replacement (THR). Hip resurfacing is intended for younger patients and athletes who do not have obesity [14]. The procedure consists of, covering femoral head with metal cap after trimming away some cortical region. Any damaged bone and cartilage within the socket are removed and replaced with a metal shell. In hip resurfacing surgery, both components are made of metal although later trends includes Poly(methyl methacrylate) ($PMMA$) coating which produce lesser wear rate.

The potential advantages of hip resurfacing compared to THR include higher bone preservation. Relatively larger femoral head size also tend to reduce the chance of dislocation. It is also considered the fact that revision surgery is much easier for any subsequent revision to a THR because a surgeon will have more original bone stock [15]. The disadvantages of hip resurfacing are chance (rate of 0–4%) of femoral neck fractures, aseptic loosening, and metal wear [15].The concept of hip resurfacing procedure is largely abandoned during 1970s and 1980s because of poor fixation techniques [16, 17].

1.2.4 Stress shielding

Bones are constantly being reshaped by osteoblasts and osteoclasts, through the continual formation and resorption of bone material. This phenomenon is first proposed by the German anatomist and surgeon Julius Wolff (1836–1902) in the 19th century. If loading on a particular bone increases, the bone will remodel itself over time to become stronger to resist that sort of loading [18, 19]. The opposite scenario also found true as well, if the load on a bone decreases, it will become weaker due to lack of stimulus for continued remodeling.

The remodeling of bone is explained by mechanotransduction, a process through which mechanical signals (here forces) are converted to biochemical signals in cellular signaling [20]. The process of mechano-transduction can be separated into four distinct steps: (1) mechanocoupling, (2) biochemical coupling, (3) transmission of signal, and (4) effector cell response [21]. It is also reported that the specific effects on bone structure depends on the duration, magnitude and rate of loading. It has also been found that only cyclic loading can induce bone formation [21]. Interstitial fluid movement within the extra cellular matrix affects the bone modeling pathways. When loaded, fluid flows away from areas of high compressive loading in the bone matrix. This lead to the hypothesize that interstitial fluid flow affects bone formation [22]. Osteocytes are the most abundant cells in bone and are also the most sensitive to such fluid flow caused by mechanical loading [20]. Upon sensing a load, osteocytes regulate bone remodeling by signaling to other cells with signaling molecules or direct contact [23]. Additionally, osteoprogenitor cells, which may differentiate into osteoblasts or osteoclasts, are also mechanosensors and may differentiate one way or another depending on the loading condition [23]. Computational studies suggest that re-orientation trabeculae in the direction of the mechanical load is is carried out by bone remodeling [24].

When the bone is replaced with the stiffer material than the bone, the implant will bear more of the load. because the bone is shielded from much of the stress being applied to the femur, the body will respond to this by increasing osteoclast activity, causing bone resorption.

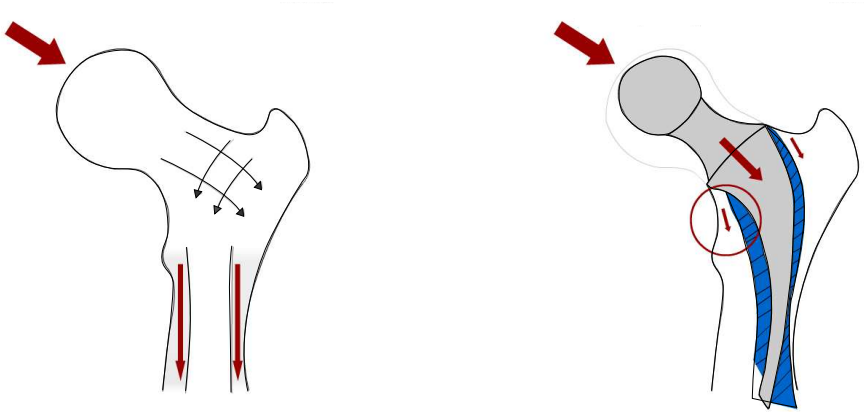

(a) Load transfer in intact bone

(b) Load transfer in implanted bone

Figure 1.5: Schematic diagram showing stress shielding. (a) in normal bone force applied on the top of femur is transmitted through the trabeculae of cancellous bone then through cortical bone. (b) in femoral implanted bone stress is transmitted through implant, so lesser stress is carried by bone.

1.2.5 Finite Element Analysis

Computer-aided design (CAD) has a variety of applications medical engineering field including prosthesis and surgical design, blood flow analysis, preoperative planning for surgeries, and computer-aided surgery. CAD tools along with finite element method geometric modeling, visualizing, analyzing the behavior of anatomical structures including human skeletal and vascular systems.This deliver a new level of understanding to engineers and medical personnel .

Finite element method (FEM) is a numerical technique for finding approximate solutions to boundary value problems for partial differential equations. Finite element Analysis (FEA) applied in different areas as a computational tool for performing engineering analysis. It uses subdivision of a whole problem domain into simpler parts, called finite elements. Finite element analysis starts with the process of dividing the model into small pieces called meshing. The behavior of each element is well-known under all possible support and load scenarios. The finite element method uses elements with different shapes. Elements share common points called nodes. After approximating the object by finite elements, the unknowns such as force and displacement associated with each node are solved.

In applying FEA, the complex problem is usually a physical system with the underlying physics such as the Euler-Bernoulli beam equation, the heat equation, or the Navier-Stokes equations expressed in either PDE or integral equations, while the divided small elements of the complex problem represent different areas in the physical system.

Accurate stress analysis of the proximal femur and pelvis are important for total hip replacements. Experimental methods often employ the use of strain gauges, which do

not provide data for the internal stress distribution. The use of a finite element model of these bones can provide valuable data on their internal stress distribution. Finite element model allows imposing realistic loading conditions, orthotropic bone properties, and accounts for the spatial variations of bone properties. The FEA results support the surgeon in finding the optimal design, size, and positioning of an implant during a preoperative design loop. This is due to the fact that an essential factor for the long-term stability of an implant is depend on the load transmission to the adjacent bone stock. An optimized femoral stem should provide bone stress patterns that closely replicate the physiological stress state in order to avoid stress shielding with the consecutive effects [25, 26].

1.3 Objectives

The objectives of the current study are as follows:

- To understand the routine activities and muscle forces associated with it from literature study.
- To create 3D models of implant and resurfacing cup usingCAD software and virtually implant it in the proximal extremity of bone geometry. This assemblies represent post-operative condition.
- To conduct the finite element analysis to understand the mechanical behavior of bone in proximal portion of femur around the implant.

1.4 Outline of Thesis

The main work of this thesis is the development of models based on the above mentioned objectives. This thesis is divided into four chapters. The main outline of all the chapters is given below:

Chapter 1: This chapter consists of overview and general information to navigate through thesis. It also includes current advances in orthopedic research.

Chapter 2: The literature review and advances associated the current study is revised in this chapter. The relevant data needed for the study is addressed and acquired.

Chapter 3: This chapter discuss the material and methods adopted for the study. $3D$ modeling of post operative geometries are discussed along with the FEM modeling.

Chapter 4: In this chapter, The finding of the study is discussed and conclusions are drawn.

Chapter 5: Summary of the whole thesis is pointed out in this chapter. The scope and future direction of work has been presented.

CHAPTER 2

Literature review

2.1 Introduction

This chapter narrates the work done by other researchers in related fields and recent advances that contribute to current investigation. The evolution in understanding of routine activities among the patients, muscle forces and hip contact force, mechanical properties of bio materials are addressed. The importance of current investigation and scope is presented.

2.2 Literature review

Evaluating patient activities is important to obtain qualitative information in assessing the clinical outcome after total hip arthroplasty [27]. Some early attempts have been made to quantify the routine activities among total hip patients and retrieve associated forces around the joints [28, 29].

Bergmann et *al.* (2001) reported the hip contacted forces during activities such as slow walking at slow speed on level ground, normal walking, fast walking on level ground, walking upstairs, walking downstairs, standing up, sitting down, two–legged stance–one-legged stance, knee bend for four patients [30].

2.2.1 Routine activities and associated forces

The knowledge about the duration of daily activity among the THA patients is important to asses the success rate of implants. Loading on the implant vary on the activity in which the patients are involved. Morlock et *al.* (2001) recorded activities of total hip

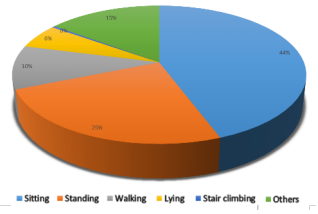

Figure 2.1: Durations and frequencies of the defined activities. The average measurement duration was just below 10 h. The most frequent activity was sitting (44.3% of the time), followed by standing (24.5%). Data reported by Morlock et *al.* (2001) [31].

patient over whole day periods. A population of 42 patients were monitored during daily living, the orientations of 2 lower leg segments were collected. Frequency and duration for common activities like walking, going up and down stairs, sitting, standing and lying were identified and recorded. Figure 2.1 shows defined activities observed by the researcher. The most frequent activity was sitting (44.3% of the time), secondly standing (24.5%), walking (10.2%), lying (5.8%) and stair climbing (0.4%) [31]. This data can serve as basis for the definition of load collectives required for testing new implants. Realistic pre-clinical testing of artificial joints is an important aspect in the improvement of durability and survival times of the implants [31].

2.3 Forces acting on proximal femur

It was proven that the success of the implant depend on the loading on the implant. Muscle loading found influences the stresses and strains in the femur and thereby affects the long term success and bone adaptation around implant. Artificial joint studied for its durability, design and survival times must be loaded with real life loading condition. Physiological loading is very crucial if bone remodeling or implant settling is simulated [32]. Computational studies with realistic physiological loading produces most accurate results in pre-clinical testing.

Some early attempts are made to calculate hip contact forces using simplified muscle models and different optimization methods [33–35]. Bergmann et *al.* (2001) reported measurements of hip contact forces with instrumented implants. Synchronous analysis of gait patterns and ground reaction forces were performed in four THA patients during the most frequent activities of daily living. Activities studied include slow walking at slower speed on level surface, normal walking, fast walking on level surface, walking upstairs, downstairs, sitting down, standing up, two–legged stance–one-legged stance, knee bend among four patients [30].

The study followed by Heller et *al.* (2001) quantitatively validate the loading conditions at proximal femur by using individual musculoskeletal models of the lower extremity [36]. The study aimed to calculate the hip contact force as well as muscle forces

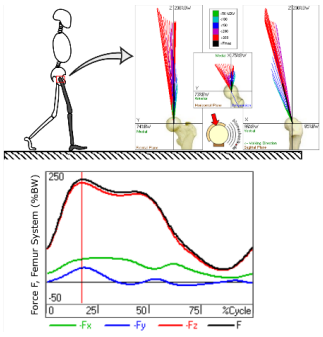

Figure 2.2: Contact force of average patients trials during normal walking. Bottom: The patient total average of F and its components $-F_x$, $-F_y$, $-F_z$. The highest value was the peak force F_p=248% BW. Top: Vector representation of contact force relative to the femur. The data is adopted from Bergmann et *al.* (2001) [30]

during walking and stair climbing for a number of patients and compared this findings with in-vivo data. The muscle and contact forces at joints are calculated using nverse dynamics and optimization algorithm. The findings provide reasonably good loading conditions for the analysis of prosthetic loading, bone remodeling adjacent to implant and fracture fixation.

The findings obtained using instrumented total hip implants with telemetric data communication system by Bergmann et *al.* (2001) is one of the most used set of data among orthopedic researchers. In the current study the force data reported by the above author was used to produce the physiological loading in CAD model.

2.3.1 Hip contact forces

Magnitude and direction of contact force acting on hip joint influences fixation stability of total hip implants. Many attempts have been made to estimate the resultant force acting on the femur. Apart from the static load, the dynamic forces are also involved in human locomotion. It may cause a load on the hip-joint will be considerably higher than the body weight. Hip joint forces can be obtained in vivo using instrumented prostheses [7, 8]. Musculoskeletal models may be employed to predict muscle forces and joint loading in a noninvasive way using inverse dynamic analysis [9, 10]. The Figure 1.3. Mathematical approach consists of lower limb musculoskeletal models usually exhibit a tendency to overestimate the hip contact forces ($HCFs$) magnitude [11]. Its also found that the magnitude and direction of the hip contact force vector depend on subject specific bone geometry [6].

Figure 2.2 shows the evolution of contact force of average THA patients during normal walking gait cycle reported by bergmann et *al.* (2001). The peak value of resultant force was observed at frame number 37. The components of forces in lateral-medial, posterior-anterior, distal-proximal directions are F_x,$F_y$and F_z respectively.

The THA patients are recommended to avoid activities that cause very steep hip contact forces. Since the torsional stability of implants may be critical the stair climbing activity is very important. Figure 2.3 shows the evolution of contact force of average patients during stair climbing reported by bergmann et *al.* (2001). The peak value of torsional moment was observed at frame number 40. The components of forces in lateral-medial, posterior-anterior, distal-proximal directions are F_x, F_y and F_z respectively.

2.3.2 Muscle forces around hip

It has been proven that that muscles are major contributors to femoral loading [32]. Due to ethical concerns the practice of invasive method to find the muscle forces were discontinued. The only remaining option to quantitatively asses the complex muscle force is by computer analysis. Heller et *al.* (2001) calculated the muscle forces among THA patients by using optimization algorithms by analysis kinetic and kinematic information [36]. The measured hip contact forces served to check the validity of calculated results.

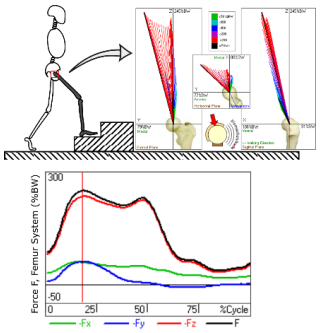

Figure 2.3: Contact force of average patient trials during stair clamping. Bottom: The patient total average of F and its components $-F_x$, $-F_y$ and $-F_z$. The highest value was the peak force F_p=265% BW. Top: Vector representation of contact force relative to the femur. The data is adopted from Bergmann et *al.* (2001) [30]

Walking

According to Heller et *al.* (2001) the muscle that were activate at peak hip contact phase of normal walking gate were abductortensor, fascia lata- proximal part,tensor fascia lata - distal partand vastus lateralis. Forces experienced at these muscles were reported as 86.5 %BW, 13.2 %BW, -19.0 %BW ,-92.9 %BW. The point of action and direction of these muscles are shown in Figure 3.4.

Stair climbing

Torsional stability of implants is challenged by activities like stair climbing. The muscle that were activate at peak hip contact phase of stair climbing gate were abductor, ilio-

tibial tract-proximal part, ilio-tibial tract-distal part, tensor fascia lata-proximal part, tensor fascia lata-distal part, vastus lateralis, vastus medialis. Forces experienced at these muscles were reported as 84.9 %BW, 12.8 %BW, -16.8 %BW, 2.9 %BW, -6.5 %BW, -135.1 %BW, -267.1 %BW. The line of action of the muscles are similar to that of walking activity however vastus lateralisand vastus medialisacts on lateral and medial part of femur respectively.

2.4 Material properties of implant and bone

The introduction of new bio material has changed the orthopedic treatment considerably. The choice of bio material depends on factors like joint anatomy, joint mechanical strength and characteristics of materials. The material properties of the femoral stem found to have effect on the fixation of implant. Weinans et *al.* (1992) studied the mechanical consequences like bone adaptation and there by long term success of different femoral stem materials using finite element method [37].

2.4.1 Alloy implant

Titanium based alloy is a best candidate for orthopedic implant because of its bio compatibility and corrosion resistance. Stress shielding very important aspect arise from the difference in flexibility or stiffness of the natural bone and implant material [38]. Titanium alloy shows relatively low young's modulus among metal implants which is another attractive property.

Pure titanium and titanium alloys are good metallic materials for biomedical applications. Ti–6Al–4V has been a main biomedical titanium alloy for a long period. Another option include β type alloys which composed of non-toxic elements. The moduli β type alloys are much less than those of $\alpha+\beta$ type alloys like Ti–6Al–4V [39]. For the current analysis the implant material is assumed to have moduli of 110 Mpa and poisson ratio of 0.3 [40].

2.4.2 Bone

The solid model of the "3rd generation composite femur" made by Pacific Research Labs, Vashon Island, WA is used in this analysis. In third-generation composite femur have the cortical bone analogue material is short glass fiber reinforced epoxy, primarily to provide better fracture and fatigue resistance. It also show increase tensile strength and modulus, compressive strength and modulus, thermal stability, and moisture resistance [41]. The mechanical properties noted by Pacific Research Laboratories cortical region is shown in table 2.1.

Table 2.1: Tensile and compressive properties of third-generation composite (3rd gen.) and natural human cortical bone (Pacific Research Laboratories, Inc., 2007)

	3rd gen.	Natural
Tensile elastic modulus (GPa)	12.4	17
Tensile strength (MPa)	90	130
Compressive elastic modulus (GPa)	7.6	17
Compressive strength (MPa)	120	170

2.5 Summary

To authors best knowledge there is no published comparison studies is done to quantitatively determine the effect of hip surgery. So the focus of the current study is to analyze the effect of total hip arthroplasty and hip resurfacing arthroplasty in proximal femur using finite element analysis. The simulation were conducted in intact and implanted models assuming perfectly bonded interface between implant and surrounding bone stock. The physiological muscle loading from the daily activities of patients is used to analyze the finite element models. The most frequently activity among the patients was walking. The stair climbing activity is also worth considering because the bending moment affects the primary fixation of implants. The muscle forces and hip contact force of the walking and stair climbing activity at specific frames was selected for analysis. Titanium and its alloys are widely used bio materials for orthopedic needs. The mechanical properties of titanium alloy was selected for finite element analysis. Cancellous and cortical region of the femur model is imposed with the mechanical properties provided by the manufacturer.

CHAPTER 3

Materials and methods

3.1 Introduction

This chapter discusses the geometric modeling technique of the implants and the finite element procedure adopted for analysis. The typical implants available these days as well as the geometrical dimensions for solid modeling with it discussed. Meshing is a critical aspect of engineering analysis. The density, transition of mesh and the quality of mesh is crucial in the finite element analysis (FEA) of models. Meshing method, localized mesh control in the geometry is addressed in this chapter. Physical behavior of the models is predicted by mechanical analysis using finite element analysis. Numerical approximation using Finite element method (FEM) is used to find the mechanical behavior of bone around implant. The boundary condition (Loads and constraints) imposed on the intact and implanted model as well as the material properties assigned is covered in this chapter.

3.2 Computer-aided design (CAD)

Computer-aided design (CAD) tools have been conventionally used for engineering design and manufacturing. Advances in information technology enabled engineers to deploy the CAD with many new and important bio-medical applications. In current study one of the most widely available CAD software in academia was used make models of implants.

A model of the third generation composite left femur ($3GCF$) (Model No.3306, pascific research laboratories, vashon, WA) was retrieved from Biomechnics European Lab-

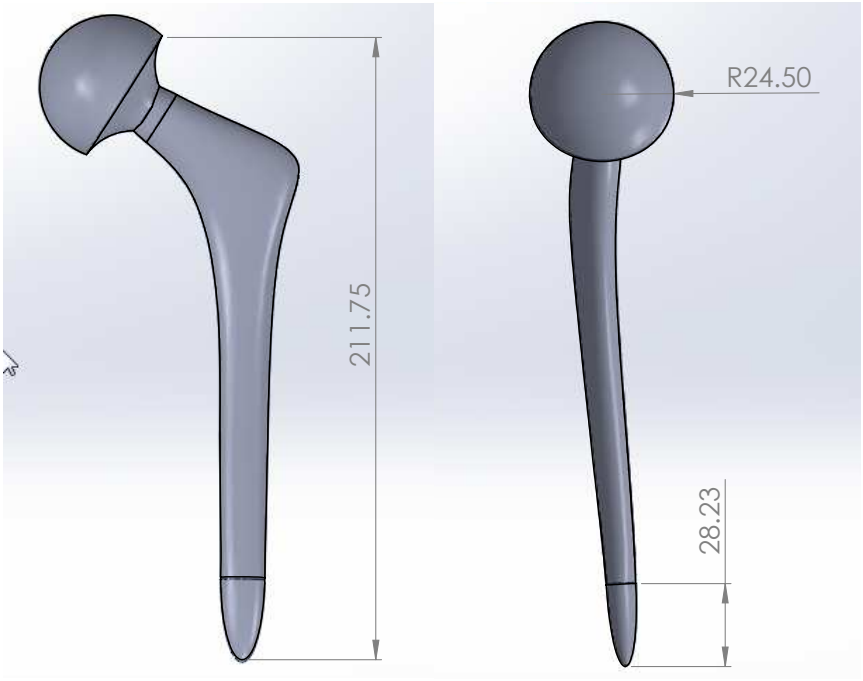

Figure 3.1: The model of endoprosthesis developed in Solidworks (Dassault Systèmes, Waltham, USA). All the dimensions are in *mm*

oratory Repository [42]. The model contains surfaces representing both cortical and cancellous bone, obtained via assembly of CT-scan slices. Third composite femur model found to give satisfactory bio-mechanical analogy of human femur and anatomical detail. The 3*GCF* bones provides uniformity in mechanical properties in cortical region. The cortical analogue is composed of short glass fiber reinforced epoxy and has improved anatomical detail than previous model [43]. The model was then loaded in Solidworks 2012 (Dassault Systèmes, Waltham, USA) for geometry cleaning. The proximal part for the analysis was retained by executing plane cutting at 240 mm from the ball head.

3.2.1 Endoprosthesis

Hip joint prosthesis are available in different shapes and materials. According to shape endoprosthesis is classified into two, short shaft prosthetic and surface prosthetic. The selection of shaft prosthesis depend on factors like anatomy of bone, age, patient activity etc.., The typical shaft prosthesis includes head, neck and shaft. A typical prosthesis consists of these parts modeled in Solidworks 2012 (Dassault Systèmes, Waltham, USA) as shown in Figure 3.1.

The shaft length and width of the implant were 112.75 mm and 12 mm respectively. The ball head of radius 24.50 mm was modeled (Figure 3.1). A slightly curved shaft de-

sign was adopted to enable perfect fit in bone model. The model of prosthesis was virtually implanted in proximal portion of the bone model to replicate the post operative geometry (Figure 3.3c).

3.2.2 The resurfacing cup

Generally the size of hip resurfacing model is little bigger than that of femur head [44]. The radius of curved surface was designed as 26.50 mm, which was bigger than head diameter of the stemmed prosthesis. The cross section was made in front plane and revolved to form the geometry. The stem was designed length 60 mm with diameter of 6 mm (Figure 3.2) .

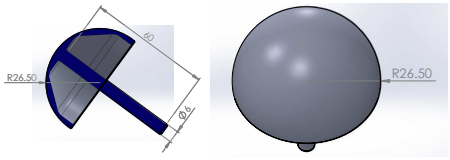

(a) (b)

Figure 3.2: The Resurfacing cup geometry developed for current study. All the dimensions are in mm

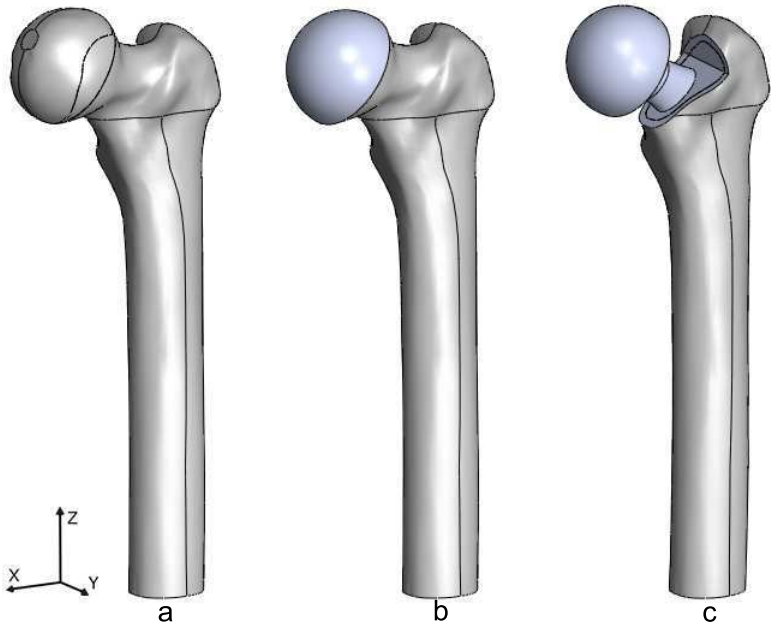

Figure 3.3: The Computer-aided designs developed of (a) intact model of left femur (b) model virtually implanted with resurfacing cup (c) model implanted with edoprosthetic

The model of prosthesis was added to bone geometry by boolean operations using *CAD* software (Figure 3.3c). The models are afterward imported to ANSYS DesignModeler interface for basic geometry cleaning and inter facial definition.

Table 3.1: Material properties assigned for Finite element modeling.

	Density(kg/m^3)	Young's modulus (Gpa)	Poisons ratio
Titanium alloy	4620	110	0.30
Cortical bone	1800	17	0.31
Cancellous bone	340	0.57	0.31

3.3 Finite element modeling (FEM)

3.3.1 Meshing the components

The accuracy of the finite element solution is dependent on the quality of the mesh. Meshed region should have proportional elements ie, the transition between mesh densities need to be smooth and gradual without distorted elements.

The models were imported to ANSYS v15.0 finite element software (ANSYS, Inc., PA, USA) and meshed with 10 nodded tetrahedral elements. SOLID187 element is the higher order $3D$, 10-node element in ANSYS. SOLID187 has a quadratic displacement behavior and is well suited for modeling irregular meshes. The element is defined by 10 nodes having three degrees of freedom at each node: translations in the nodal x, y, and z directions [45]. For the simplified femur model, that tetrahedral linear element more close results to analytical ones, but hexahedral quadratic elements found to have less effect to the degree of refinement of the mesh [46].

Patch confirming meshing algorithm was employed to with proximal refinement to generate a globally smooth mesh. The mesh size for cancellous and cortical region is set to be 2.5 mm and 3 mm respectively according to mesh convergence study. The resulting model of intact model consists of 47895 and 40498 elements for cortical and intramedullary region respectively. The number of elements for resurfacing cup and endoprosthesis model was about 3428 and 8743 respectively. The implant bone interface was defined as fully bonded with the bone using six nodded surface to surface contact element [47].

3.3.2 Material properties

Titanium alloys exhibits lower modulus, superior biocompatibility and enhanced corrosion resistance when compared stainless steels and cobalt-based alloys. Resurfacing cup and endoprosthesis assumed to be made of titanium alloys and assumed to have young's modulus of 110 Gpa [40]. The material properties of bone are assumed to be linear elastic and isotropic the material distribution was modeled as homogeneous throughout the bone. The Poisson's ratio was assumed to be 0.3 for all materials. The Young's modulus of 17 Gpa and 570 Mpa was assigned for cortical and cancellous bone region [48]. The material properties assigned in the finite element modeling is listed in table 3.1.

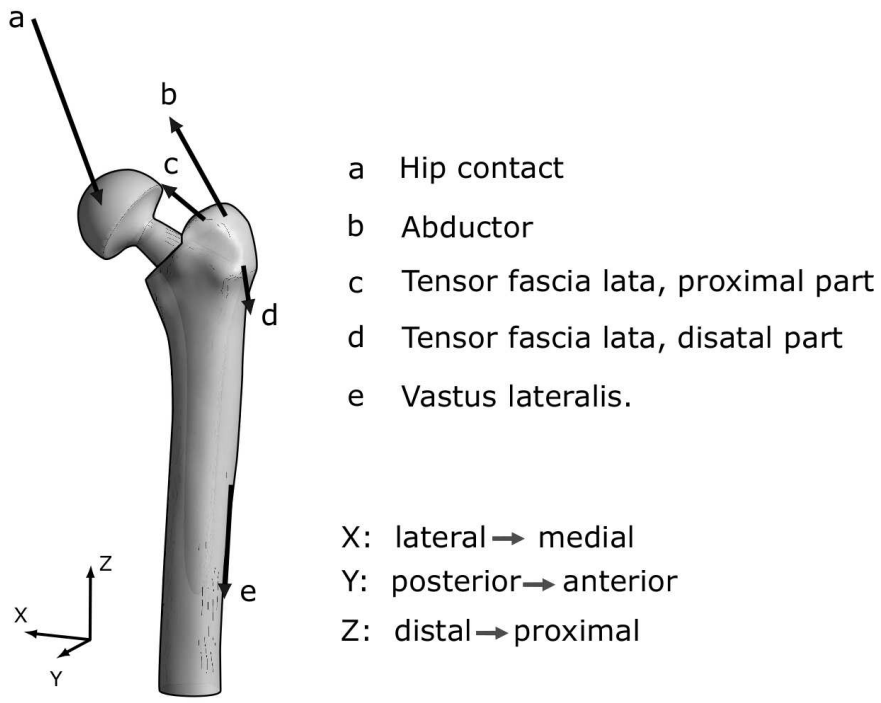

Figure 3.4: Simplified loading configuration for walking with highest hip contact force. The point of action of the muscle force and hip contact force are represented as vectors in schematic.

3.3.3 Boundary condition (Loads and constraints)

Imposing physiological loading condition from routine activities of *THA* patient is important to understand the stress sheilding. Loading configuration on the finite element model found to produce important role in the simulation outcome [49]. The hip contact force and associated muscle force from daily activities among THA patients is used for analysis of the computer models. It is also found that the changes in joint geometry may results in the change in hip contact force vector during gait cycle [6]. The hip contact force and associated muscle force data of the hip patients during routine activities was adopted from Bergmann et *al.* (2001) [30, 36]. The muscle forces and hip contact force are calculated by assuming a body weight of 65 kg which is an approximate weight of population. The peak average hip contact force was observed at frame number 37 for normal walking. The forces associated with this is listed in table 3.2. The boundary conditions applied for normal walking simulation is shown in Figure 3.4. The distal part of the femur was kept fixed and forces are directly applied to nodes. The maximum torsional moment observed at frame number 40 of stair climbing action. The associated muscle forces are listed in table table 3.3.

The maximum torque was observed in stair climbing action at frame number 40 among THA patients [30]. The active muscles and forces produced by it listed in table 3.3. Apart from the muscles listed in table 3.2 ilio-tibial tract proximal partand ilio-

Table 3.2: Force components F_x, F_y and F_z in femur co ordinate system at peak hip contact frame of normal walking.

Force (N)	Normal walking		
	F_x	F_y	F_z
Hip contact	−344.33	−209.15	−1461.49
Abductor	369.84	27.42	551.57
Tensor fascia lata, proximal part	45.91	73.97	84.17
Tensor fascia lata, distal part	−3.19	−4.46	−121.15
Vastus lateralis	−5.74	117.97	−592.38

Table 3.3: Force components F_x, F_y and F_z in femur co ordinate system at peak torsional moment of Stair climbing.

Force (N)	Stair Climbing		
	F_x	F_y	F_z
Hip contact	−378.13	−386.42	−1506.77
Abductor	446.99	183.64	541.36
Ilio-tibial tract, proximal part	66.95	−19.13	81.62
Ilio-tibial tract, distal part	−3.19	−5.1	−107.13
Tensor fascia lata, proximal part	19.77	31.24	18.49
Tensor fascia lata, distal part	−1.28	−1.91	−41.45
Vastus lateralis	−14.03	142.84	−861.47
Vastus medialis	−56.11	252.51	−1703.16

tibial tract, distal part contribute to the physiological loading condition. These muscle forces are applied to its anatomical location in intact, periprosthetic and resurfaced bone model. These models were then solved using Newton-Raphson iterative scheme in ANSYS.

3.4 Summary

The *CAD* geometry representing intact bone as well as post operative condition was modeled in Solidworks 2012. Post operative geometry includes resurface bone geometry and periprosthetic femur geometry. Appropriate meshing technique was employed to ensure good quality result and contact behavior was defined. Material properties of bone and metal implant was assigned. The models are solved for fixed boundary condition and muscle forces both for walking and stair climbing. The stress distribution in the bone was analyzed in post processing to draw conclusion.

CHAPTER 4

Results and discussion

4.1 Introduction

This chapter discuss the outcome of the finite element analysis (FEA). Pre operative and post operative geometries were analyzed and the conclusions are drawn. The stress distribution in the bone stock around the implant is plotted and the load transfer across the bone model is studied. The result of the study is correlated with the outcome of other researchers work. The effect of the implantation in the bone mineral density is discussed.

4.2 Stress distribution in bone stock

In order to assess the changes in load transfer due total hip arthroplasty and resurfacing procedure, von Mises stress distributions in the intact, implanted and resurfaced femoral models are calculated in elements. The main finding are reported in the following sections.

4.2.1 Intact femur model

The intact model is found to experience more of uniform stress through out the domain. Figure 4.1 shows the stress distribution in cortical bone region. For normal walking loading condition the maximum stress in the intact model was found as 44.54 MPa. For stair climbing the maximum stress of 46.26 MPa was observed at cortical region. The minimum stress were 0.0160 MPa and 0.0182 MPa in cancellous bone region for walking and stair climbing activities respectively.

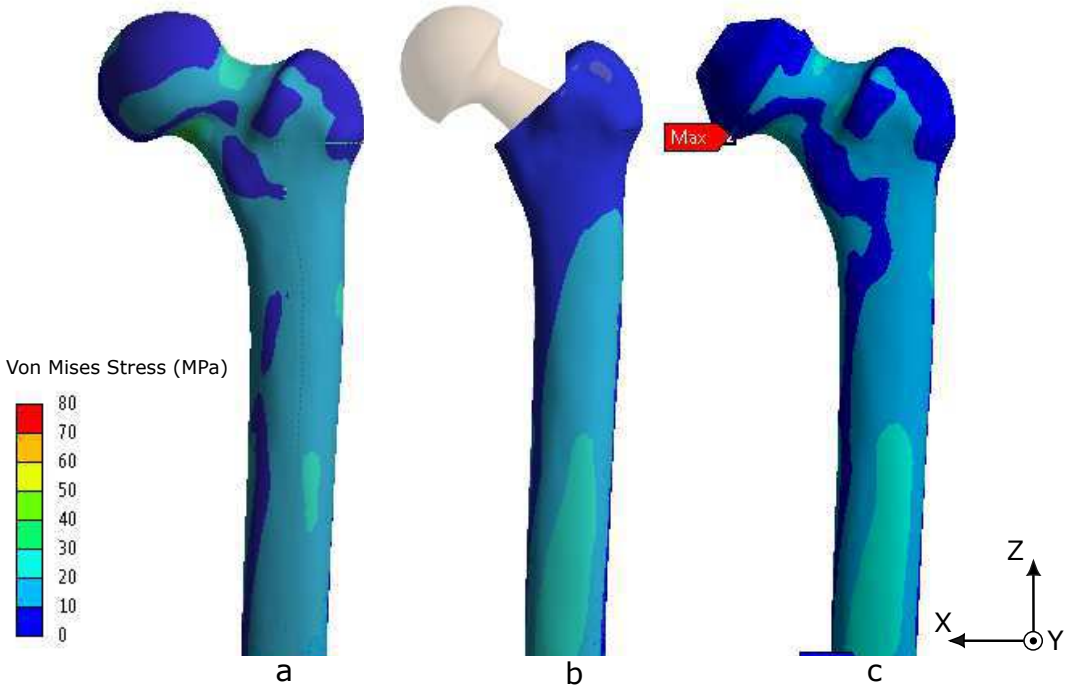

Figure 4.1: The von Mises stress distribution in cortical bone region of proximal femur models (a) intact model of left femur (b) model implanted with edoprosthetic (c) model virtually implanted with resurfacing cup.

In the intact femur, the higher stress is found vicinity of the neck region in medal side (Figure 4.2). Figure 4.2 also indicate that the load is transferred from the medial lateral direction to posterior anterior direction as move towards distal end of femur. Figure 4.3 shows the stresses in the bone stock greater than 5MPa. The Physiological stress distribution in the intact bone is evident from Figure 4.3a.

4.2.2 Implanted femur model

The implanted model found to have drastic change in stress distribution and load transfer (4.2). For normal walking loading condition the maximum stress in the implanted model was found as 46.55 MPa. For stair climbing the maximum stress of 54.68 MPa was observed at cortical region. The minimum stress were 0.0105 MPa and 0.0102 MPa in cancellous bone region for walking and stair climbing activities respectively.

The load is transferred from the medial lateral direction to posterior anterior direction as move towards distal end of femur like in intact case however the medial lateral parts found to experience lesser stress (Figure 4.1b). The trochanter region found to experience very lesser von mises stress as shown in Figure 4.3.

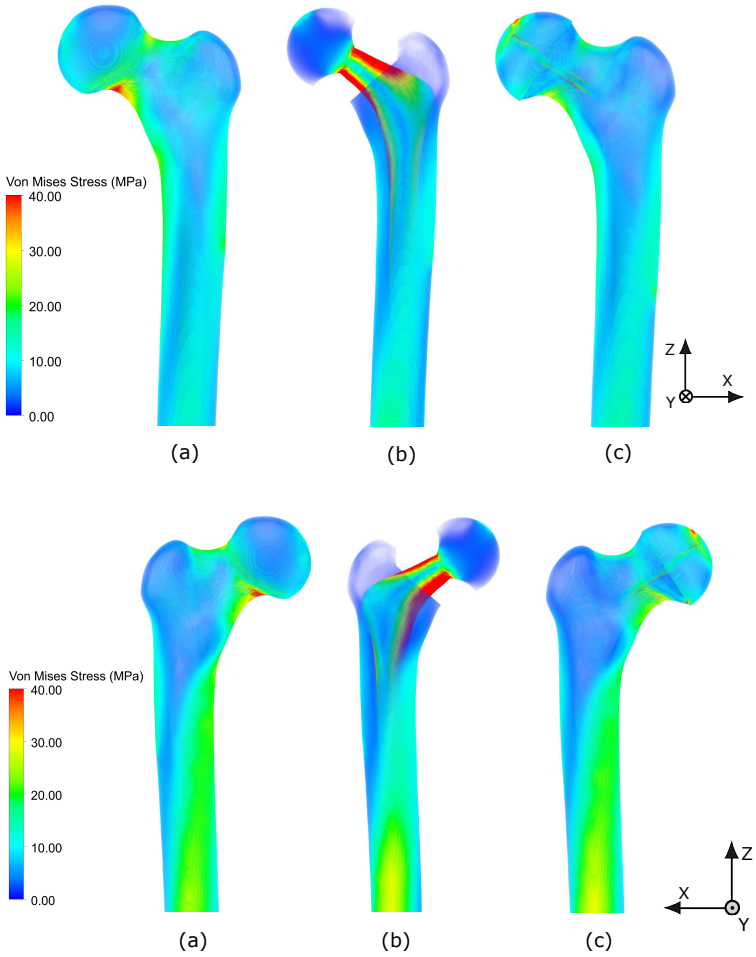

Figure 4.2: The volume rendering of von Mises stress distribution in proximal femur models, anterior and posterior view respectively. Applied loading condition correspond to the instant peak hip contact forces during stance phase of gait.

4.2.3 Resurfaced femur model

The bone stock of resurfaced femur model found to have very similar stress distribution (Figure 4.1). For normal walking loading condition the maximum stress in the implanted model was found as 52.35 MPa. For stair climbing the maximum stress of 70.01 MPa was observed at cortical region. The minimum stress were 0.0138 MPa and 0.0192 MPa in cancellous bone region for walking and stair climbing activities respectively.

The load transfer is noticed from the medial lateral direction to posterior anterior direction as move from proximal end towards distal end of femur (Figure 4.1c). The results also shows a very high stress concentration in the medial part of the neck region (Figure 4.3).

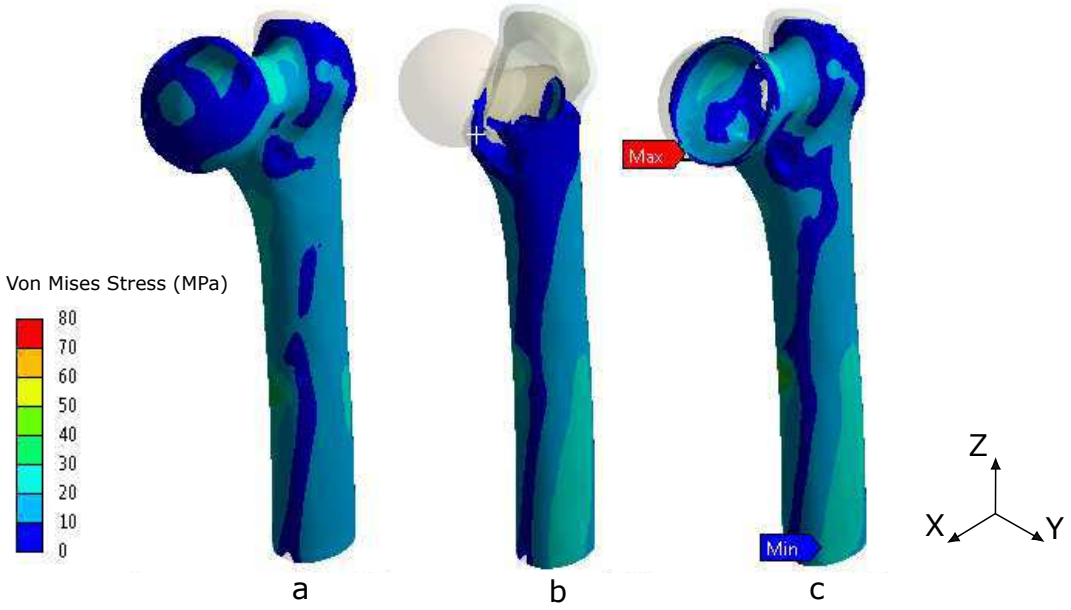

Figure 4.3: The stress distribution in the (a) intact femur, (b) implanted femur and (c) resurfaced femur model showing stresses greater than 5MPa

4.3 Comparison of results

The post processing of the model were conducted to compare the load transfer across the proximal femur, stress shielding. Average stresses in specific regions was found out for the ease of comparison. In general the the stress distribution is found to be very similar walking and stair climbing action however little higher stress is found to experience in later case. The findings are discussed in following sections.

4.3.1 Load transfer across the proximal femur

The physiological load transfer was observed in intact bone model. The load was found transferred from proximal end to distal end through the cortical bone region (Figure 4.1). Figure 4.5 and Figure 4.6 represents the stress distribution at different sections of the bone. The load transfer through the resurfaced cup model is found very similar, however the load was found shared between cortical region and cancellous region.

The anterior posterior section helps to understand the interaction of implanted material in surrounding bone and the load transfer through it.(Figure 4.4). Again in intact and resurfaced cup femur experienced almost similar stress distribution so the similar load transfer. For implanted model predominant drop in stress level is observed in medial side and greater trochanter region.

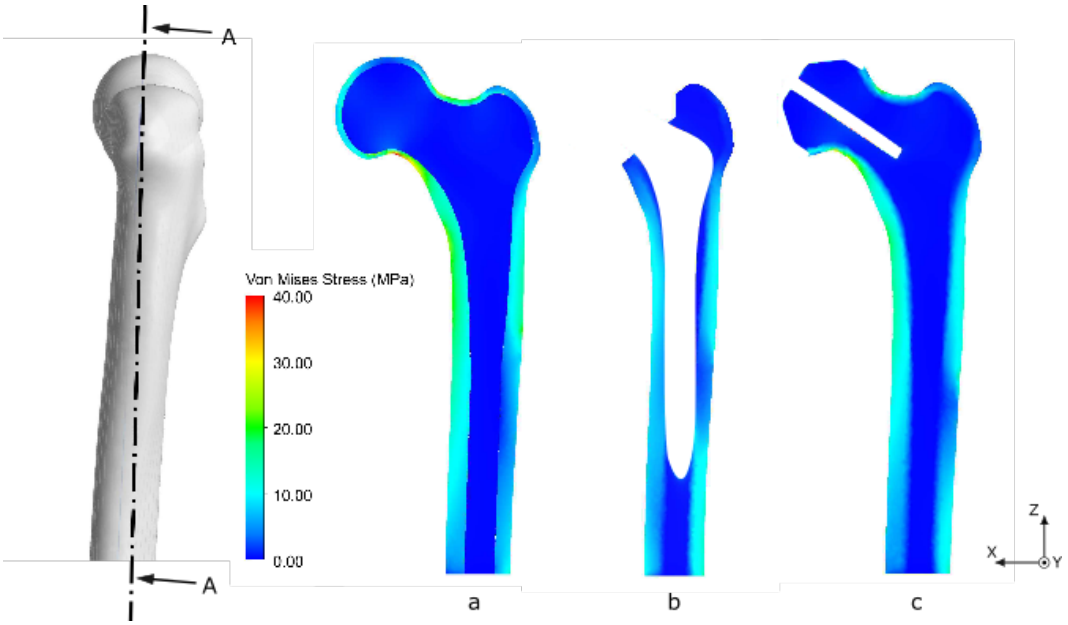

Figure 4.4: Stress distribution in anterior-posterior section of the models.

4.3.2 Stress shielding

The post operative stress distribution in the femur is compared with the intact model in Figure 4.2. The stress distribution was found to be similar in intact and resurfaced cup models. Pronounced bending pattern found in mediolateral direction in proximal part in both models. Load pattern was then shifted towards anterioposterior direction when move to distal end, with higher stress at the rigidly fixed end. In case of periprosthetic femur drastic drop in stress levels was found in greater trochanter, lesser trochanter and third trochanter regions. Decreased stresses was found in mediolateral direction as well. In case of loading condition correspond to maximum torque in stair climbing case the stress experienced by the bone was little higher otherwise distribution was found to be very similar.

4.3.3 Average stresses in gruen zones

The bone region around the implant was divided into 7 zones in order to determine the changes [50]. The average value of the von mises stresses were quantified for the conventional 7 gruen zones. The relative change of the stresses each zone was calculated. Figure 4.7 shows the average stress found in corresponding region in bone around implant. The average stresses in region intact bone was 3 Mpa to 9 Mpa. Zones 6 and 7 found to have prevailing stress difference compared to post operative cases.

The resurfaced geometry found to have very negligible difference in stresses in bone stock in zones 1 to 4 however the the decrease in stress in zones 5, 6, 7 were 31.06 %, 53.95% and 75.29% respectively.

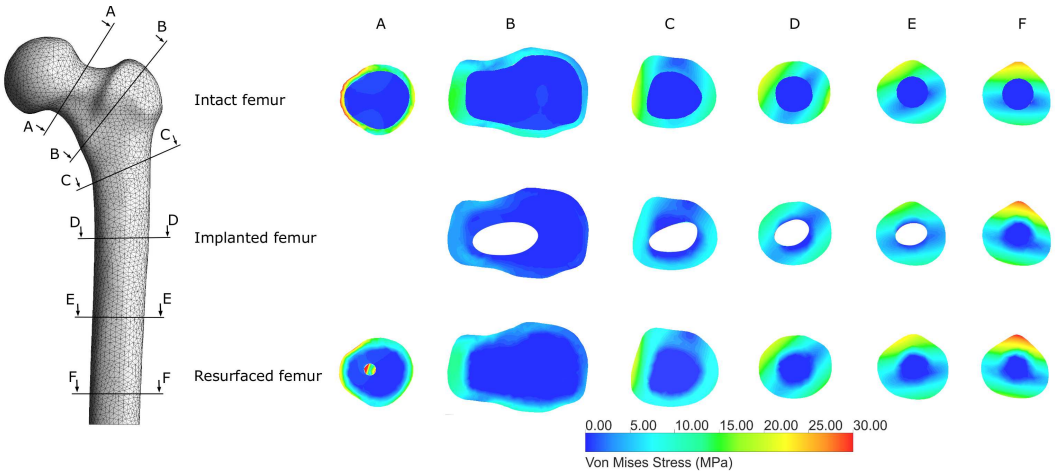

Figure 4.5: The von Mises stress distribution at different sections in proximal part femur. Applied loading condition correspond to the instant peak hip contact forces during normal walking .

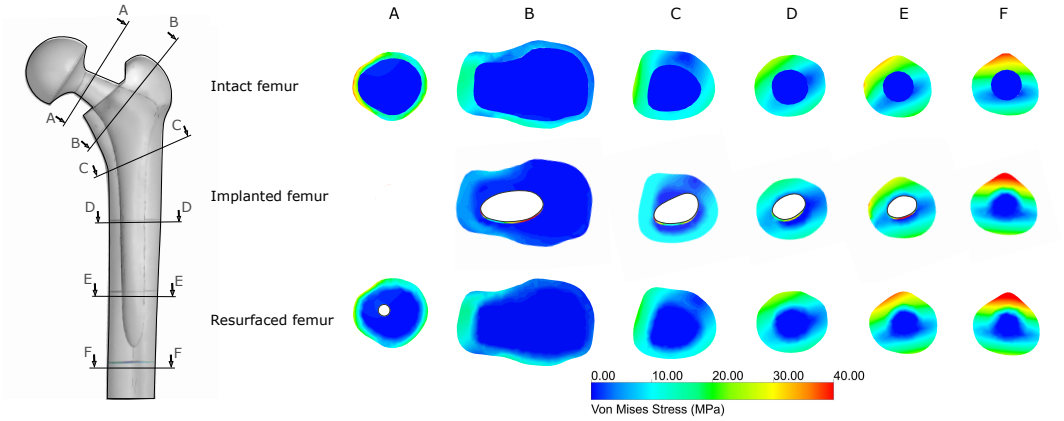

Figure 4.6: The von Mises stress distribution at different sections in proximal part femur. Applied loading condition correspond to the instant peak hip contact forces during stair climbing activity.

Bone stock in implanted geometry found to have relatively higher stresses in region 2 and 3 than that of intact geometry. Likewise in resurfaced implant drop of average von-mises stress was observed in medial side. The decrease stress in zones 5, 6, 7 were 14.08%, 47.97% and 40.73% respectively.

4.4 Discussion

The aim of the study was to investigate the effect of surgery in proximal femur using finite element analysis. The three dimensional model of intact, implanted and resurfaced cup model were used for analysis. The simulation were conducted assuming perfectly bonded interface between implant and surrounding bone stock. The maximum stresses was found in medial lateral sides of the models and it is very comparable with other computational studies [51, 52]. The maximum von mises stresses in both implants were

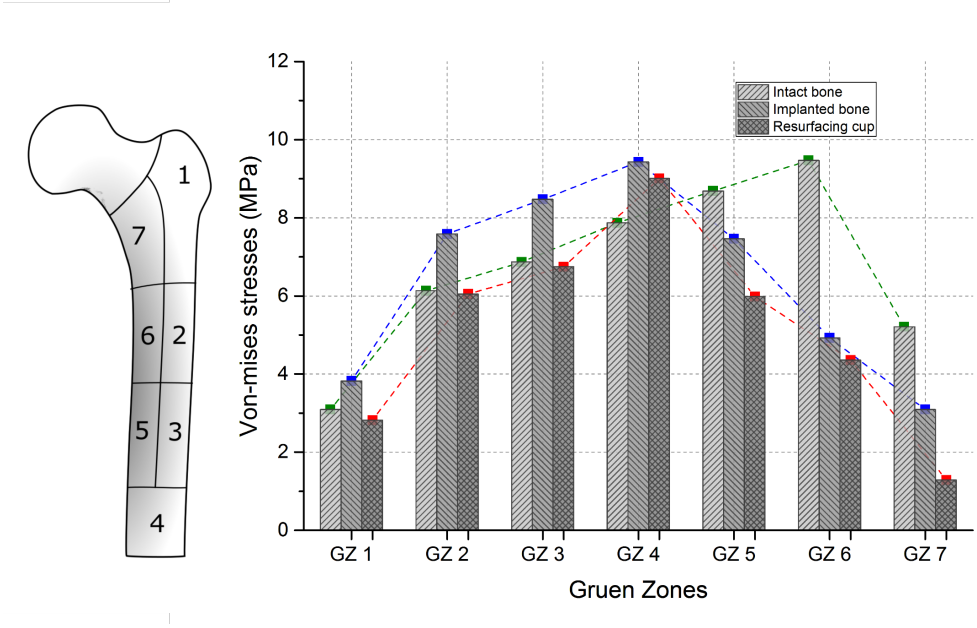

Figure 4.7: The average von mises stresses (MPa) in each Gruen zones for peak hip contact force during stance phase of gait.

ranged from 80 to 130. The load transfer is noticed from the medial lateral direction to posterior anterior direction as move from proximal end towards distal end of femurhich were far below the failure strength of the implant material (Titanium alloy).

The load transfer was noticed from the medial lateral direction to posterior anterior direction as move from proximal end towards distal end of femur. Some studies shows that the stress distribution can be in medial lateral sides itself. The stress distribution is depend on subject specific geometry [52].

The resurfaced model was found to experience higher stress an neck region. This indicate the risk of femoral neck fracture in model. Some early studies suggested that femoral neck notching is the cause of the most of femoral neck fractures [53]. The notching tend to reduce the proximal femoral strength in hip resurfacing surgeries.

Some studies predicted the extent of bone mineral density after THA [49, 50]. The bone remodeling suggested is found to be a phenomena driven by mechanical stimulus. The bone adaptation based on stress and strain parameters were found to be good in predicating BMD distribution after THA surgery. Jonkers et al. (2008) studied the effect of bone mineral density (BMD) on subject specific bone geometry and loading condition. The stress distribution found to be depend on subject specific geometry [52]. The von mises stress distribution in femur model of subject 2 of the study is found to have some extent of similarity with current study (Figure 4.2). Figure 4.8 shows the average von mises stress in the gruen zones in both study. It is evident from the chart that change the average von mises stress in region 3 to 5 is relatively negligible. The current study shows the average stress in region 1, 2 and 7 is less than that of observed in jonkers et al. subject 2. According to jonkers et al. the large change in the von- mises stress was

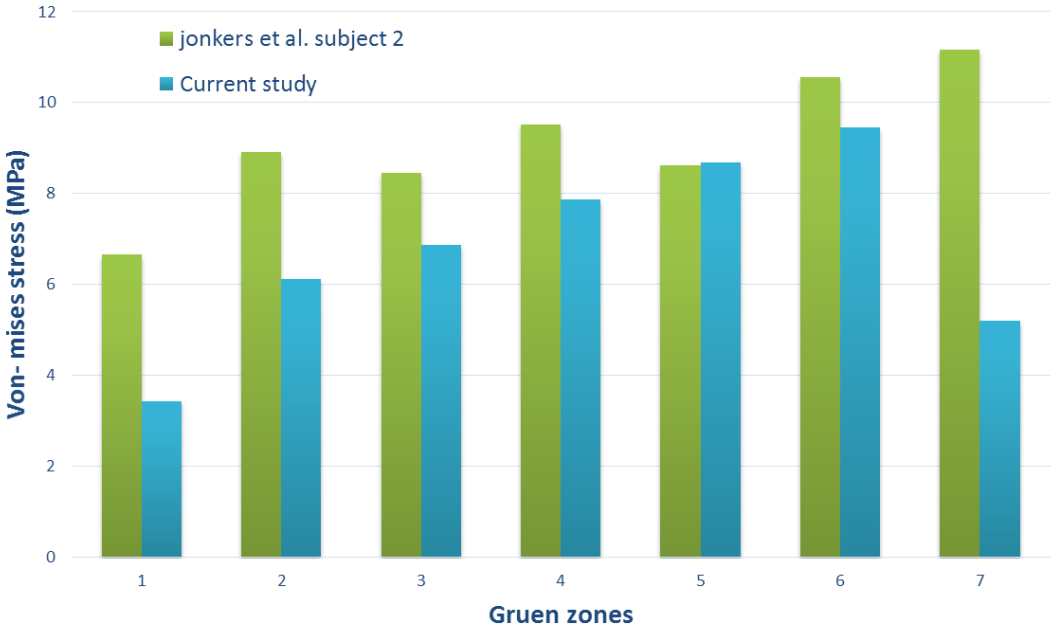

Figure 4.8: The comparison of average von mises stresses (MPa) in each Gruen zones in preoperative bone model of current study with that of Jonkers et *al.* (2008).

observed in gruen zone 7. The BMD measurements displayed the prominent decrease in mineral density found in Gruen zone 7. The researcher also observed slight increase in BMD gruen zones 1 and 4 where a slight change in stress is observed. In short 3D stress distribution arise from subject specific loading condition was found responsible for the BMD changes after THR [52].

4.5 Summary

The goal of the current study was to analyze the effect of total hip arthroplasty and hip resurfacing arthroplasty in proximal femur using finite element analysis. The simulation were conducted in intact and implanted models assuming perfectly bonded interface between implant and surrounding bone stock. The maximum von mises stresses in both implants were ranged from 80 to 130 which were far below the failure strength of the implant material (Titanium alloy). The numerical studies shows predominant change in physiological stress distribution in implanted bone model. The anterior and posterior regions trochanter found to have very less stress experienced compared to implanted model. This may lead to stress shielding and subsequent bone adaptation in these particular region. Resurfaced cup model found to retain the physiological load transfer across the femur at its most extend. The study was compared against other researchers work and found correlation in the findings.

CHAPTER 5

Conclusion

This research consists of two parts — (i) Development of model to represent the pre and post operative surgical condition and (ii) Study the mechanical behavior of bone around the implant.

Development of pre and post operative models

The CAD geometry representing intact bone as well as post operative condition was modeled in Solidworks 2012. Post operative geometry includes resurface bone geometry and periprosthetic femur geometry. Appropriate meshing technique was employed to ensure good quality result and contact behavior was defined. Material properties of bone and metal implant was assigned. The models are solved for fixed boundary condition and muscle forces both for walking and stair climbing. The stress distribution in the bone was analyzed in post processing to draw conclusion.

Finite element analysis

Finite element analysis is conducted to quantify the effect of total hip arthroplasty and hip resurfacing arthroplasty in proximal femur. The simulation were conducted in intact and implanted models assuming perfectly bonded interface between implant and surrounding bone stock. The maximum von mises stresses in both implants were ranged from 80 to 130 which were far below the failure strength of the implant material (Titanium alloy). The numerical studies shows predominant change in physiological stress distribution in implanted bone model. The anterior and posterior regions trochanter found to have very less stress experienced compared to implanted model. This may lead to stress shielding and subsequent bone adaptation in these particular region. Resur-

faced cup model found to retain the physiological load transfer across the femur at its most extend. The study was compared against other researchers work and found correlation in the findings.

5.1 Limitations and Recommendations

The current model adopted for the numerical analysis may not fully replicate the bone behavior. The $3D$ geometry made of CT slices with mechanical properties of elements defined based on BMD value produce more realistic results. The current analysis was based on liner isotropic behavior of bone material but unique structure of bone give raise to directional dependent mechanical properties. Use of static loading in single leg stance of gait also limits the generalization of these findings.

Bibliography

[1] H. Gray, Anatomy of the human body, Philadelphia: Lea & Febiger, 1918.

[2] F. Netter, The Ciba collection of medical illustrations : a compilation of pathological and anatomical paintings, Ciba Pharmaceutical Products, Summit, N.J, 1959.

[3] J. Silverstein, J. Moeller, M. Hutchinson, Common issues in orthopedics, Textbook of Family Medicine. 8th ed. Philadelphia, Pa: Saunders Elsevier.

[4] C. Gdyczynski, A. Manbachi, S. Hashemi, B. Lashkari, R. Cobbold, On estimating the directionality distribution in pedicle trabecular bone from micro-ct images, Physiological Measurement 35 (12) (2014) 24–55.

[5] F. Moller, Bevaegeapparatets anatomi, Munksgaard Danmark, Kbh, 2001.

[6] G. Lenaerts, F. D. Groote, B. Demeulenaere, M. Mulier, G. V. der Perre, A. Spaepen, I. Jonkers, Subject-specific hip geometry affects predicted hip joint contact forces during gait, Journal of Biomechanics 41 (6) (2008) 1243 – 1252.

[7] W. Hodge, R. Fijan, K. Carlson, R. Burgess, W. Harris, R. Mann, Contact pressures in the human hip joint measured in vivo, Proceedings of the National Academy of Sciences of the United States of America 83 (9) (1986) 2879–2883.

[8] B. Stansfield, A. Nicol, J. Paul, I. Kelly, F. Graichen, G. Bergmann, Direct comparison of calculated hip joint contact forces with those measured using instrumented implants. an evaluation of a three-dimensional mathematical model of the lower limb, Journal of Biomechanics 36 (7) (2003) 929–936.

[9] D. Pedersen, R. Brand, D. Davy, Pelvic muscle and acetabular contact forces during gait, Journal of Biomechanics 30 (9) (1997) 959–965.

[10] B. Stansfield, A. Nicol, Hip joint contact forces in normal subjects and subjects with total hip prostheses: Walking and stair and ramp negotiation, Clinical Biomechanics 17 (2) (2002) 130–139.

[11] L. Modenese, A. Gopalakrishnan, A. Phillips, Application of a falsification strategy to a musculoskeletal model of the lower limb and accuracy of the predicted hip contact force vector, Journal of Biomechanics 46 (6) (2013) 1193 – 1200.

[12] H. Malchau, P. Herberts, T. Eisler, G. Garellick, P. Söderman, The swedish total hip replacement register, The Journal of Bone & Joint Surgery 84 (suppl 2) (2002) S2–S20.

[13] C. Engh, J. Bobyn, A. Glassman, Porous-coated hip replacement. the factors governing bone ingrowth, stress shielding, and clinical results, Journal of Bone & Joint Surgery, British Volume 69 (1) (1987) 45–55.

[14] M. A. Mont, T. M. Seyler, S. D. Ulrich, P. E. Beaule, H. S. Boyd, M. J. Grecula, V. M. Goldberg, W. R. Kennedy, D. R. Marker, T. P. Schmalzried, et al., Effect of changing indications and techniques on total hip resurfacing., Clinical orthopaedics and related research 465 (2007) 63–70.

[15] M. A. Mont, P. S. Ragland, G. Etienne, T. M. Seyler, T. P. Schmalzried, Hip resurfacing arthroplasty, Journal of the American Academy of Orthopaedic Surgeons 14 (8) (2006) 454–463.

[16] T. P. Schmalzried, V. A. Fowble, K. J. Ure, H. C. Amstutz, Metal on metal surface replacement of the hip: Technique, fixation, and early results., Clinical orthopaedics and related research 329 (1996) S106–S114.

[17] H. Amstutz, E. Sparling, P. Grigoris, P. Campbell, F. Dorey, Surface replacement: the hip replacement of the future?, Hip international 8 (1998) 187–207.

[18] H. M. Frost, Wolff's law and bone's structural adaptations to mechanical usage: an overview for clinicians, The Angle Orthodontist 64 (3) (1994) 175–188.

[19] C. Ruff, B. Holt, E. Trinkaus, Who's afraid of the big bad wolff?wolff's law and bone functional adaptation, American journal of physical anthropology 129 (4) (2006) 484–498.

[20] C. Huang, R. Ogawa, Mechanotransduction in bone repair and regeneration, The FASEB Journal 24 (10) (2010) 3625–3632.

[21] R. Duncan, C. Turner, Mechanotransduction and the functional response of bone to mechanical strain, Calcified tissue international 57 (5) (1995) 344–358.

[22] C. Turner, M. Forwood, M. Otter, Mechanotransduction in bone: do bone cells act as sensors of fluid flow?, The FASEB Journal 8 (11) (1994) 875–878.

[23] J.-H. Chen, C. Liu, L. You, C. A. Simmons, Boning up on wolff's law: mechanical regulation of the cells that make and maintain bone, Journal of biomechanics 43 (1) (2010) 108–118.

[24] R. Huiskes, R. Ruimerman, G. H. Van Lenthe, J. D. Janssen, Effects of mechanical forces on maintenance and adaptation of form in trabecular bone, Nature 405 (6787) (2000) 704–706.

[25] M. Bessho, I. Ohnishi, J. Matsuyama, T. Matsumoto, K. Imai, K. Nakamura, Prediction of strength and strain of the proximal femur by a ct-based finite element method, Journal of Biomechanics 40 (8) (2007) 1745 – 1753.

[26] J. Simoes, M. Vaz, The influence on strain shielding of material stiffness of press-fit femoral components, Proceedings of the Institution of Mechanical Engineers, Part H: Journal of Engineering in Medicine 216 (5) (2002) 341–346.

[27] P. E. Beaula, F. J. Dorey, R. Hoke, M. LeDuff, H. C. Amstutz, The value of patient activity level in the outcome of total hip arthroplasty, The Journal of Arthroplasty 21 (4) (2006) 547 – 552.

[28] D. Kilgus, F. Dorey, G. Finerman, H. Amstutz, Patient activity, sports participation, and impact loading on the durability of cemented total hip replacements, Clinical Orthopaedics and Related Research (269) (1991) 25–31, cited By 109.

[29] G. Bergmann, F. Graichen, A. Rohlmann, Hip joint loading during walking and running, measured in two patients, Journal of Biomechanics 26 (8) (1993) 969 – 990.

[30] G. Bergmann, G. Deuretzbacher, M. Heller, F. Graichen, A. Rohlmann, J. Strauss, G. Duda, Hip contact forces and gait patterns from routine activities, Journal of Biomechanics 34 (7) (2001) 859 – 871.

[31] M. Morlock, E. Schneider, A. Bluhm, M. Vollmer, G. Bergmann, V. MÃŒller, M. Honl, Duration and frequency of every day activities in total hip patients, Journal of Biomechanics 34 (7) (2001) 873 – 881.

[32] G. N. Duda, M. Heller, J. Albinger, O. Schulz, E. Schneider, L. Claes, Influence of muscle forces on femoral strain distribution, Journal of Biomechanics 31 (9) (1998) 841 – 846.

[33] R. Crowninshield, R. Johnston, J. Andrews, R. Brand, A biomechanical investigation of the human hip, Journal of Biomechanics 11 (1978) 75 – 85.

[34] H. RÃ¶hrle, R. Scholten, C. Sigolotto, W. Sollbach, H. Kellner, Joint forces in the human pelvis-leg skeleton during walking, Journal of Biomechanics 17 (6) (1984) 409 – 424.

[35] R. A. Brand, D. R. Pedersen, D. T. Davy, G. M. Kotzar, K. G. Heiple, V. M. Goldberg, Comparison of hip force calculations and measurements in the same patient, The Journal of Arthroplasty 9 (1) (1994) 45 – 51.

[36] M. Heller, G. Bergmann, G. Deuretzbacher, L. DÃŒrselen, M. Pohl, L. Claes, N. Haas, G. Duda, Musculo-skeletal loading conditions at the hip during walking and stair climbing, Journal of Biomechanics 34 (7) (2001) 883 – 893.

[37] H. Weinans, R. Huiskes, H. J. Grootenboer, Effects of material properties of femoral hip components on bone remodeling, Journal of Orthopaedic Research 10 (6) (1992) 845–853.

[38] D. R. Sumner, J. O. GALANTE, Determinants of stress shielding: design versus materials versus interface., Clinical orthopaedics and related research 274 (1992) 202–212.

[39] M. Niinomi, Mechanical properties of biomedical titanium alloys, Materials Science and Engineering: A 243 (2) (1998) 231 – 236.

[40] M. Long, H. Rack, Titanium alloys in total joint replacement a materials science perspective, Biomaterials 19 (18) (1998) 1621–1639.

[41] A. D. Heiner, Structural properties of fourth-generation composite femurs and tibias, Journal of Biomechanics 41 (15) (2008) 3282 – 3284.

[42] P. Z. Marcello Papini, Third generation composite femur with intramedullary canal,from: The bel repository (February 2005).
URL http://www.tecno.ior.it/VRLAB/

[43] L. Cristofolini, M. Viceconti, A. Cappello, A. Toni, Mechanical validation of whole bone composite femur models, Journal of Biomechanics 29 (4) (1996) 525 – 535.

[44] F. D. Naal, M. S. Kain, O. Hersche, U. Munzinger, M. Leunig, Does hip resurfacing require larger acetabular cups than conventional tha?, Clinical orthopaedics and related research 467 (4) (2009) 923–928.

[45] I. ANSYS, Theory reference for the mechanical apdl and-mechanical applications, ANSYS INC. http://orange. engr. ucdavis. edu/Documentation12. 0/120/ans_thry. pd.

[46] A. Ramos, J. Simaues, Tetrahedral versus hexahedral finite elements in numerical modelling of the proximal femur, Medical Engineering & Physics 28 (9) (2006) 916 – 924.

[47] A. Shirazi-Adl, M. Dammak, G. Paiement, Experimental determination of friction characteristics at the trabecular bone/porous-coated metal interface in cementless implants, Journal of biomedical materials research 27 (2) (1993) 167–175.

[48] J. Stolk, N. Verdonschot, R. Huiskes, Hip-joint and abductor-muscle forces adequately represent in vivo loading of a cemented total hip reconstruction, Journal of Biomechanics 34 (7) (2001) 917–926.

[49] C. Bitsakos, J. Kerner, I. Fisher, A. A. Amis, The effect of muscle loading on the simulation of bone remodelling in the proximal femur, Journal of biomechanics 38 (1) (2005) 133–139.

[50] T. A. GRUEN, G. M. MCNEICE, H. C. AMSTUTZ, " modes of failure" of cemented stem-type femoral components: a radiographic analysis of loosening., Clinical Orthopaedics and Related Research 141 (1979) 17–27.

[51] S. Gupta, B. Pal, A. M. New, The effects of interfacial conditions and stem length on potential failure mechanisms in the uncemented resurfaced femur, Annals of biomedical engineering 38 (6) (2010) 2107–2120.

[52] I. Jonkers, N. Sauwen, G. Lenaerts, M. Mulier, G. Van der Perre, S. Jaecques, Relation between subject-specific hip joint loading, stress distribution in the proximal femur and bone mineral density changes after total hip replacement, Journal of biomechanics 41 (16) (2008) 3405–3413.

[53] A. Shimmin, D. Back, Femoral neck fractures following birmingham hip resurfacing a national review of 50 cases, Journal of Bone & Joint Surgery, British Volume 87 (4) (2005) 463–464.